ACS Chemical Neuroscience

Article

Identification of specific ligand-receptor interactions that govern binding and cooperativity of diverse modulators to a common metabotropic glutamate receptor 5 allosteric site

KAREN JOAN GREGORY, Elizabeth D Nguyen, Chrysa Malosh, Jeffrey L Mendenhall, Jessica Z Zic, Brittney S Bates, Meredith J Noetzel, Emma F Squire, Eric M Turner, Jerri M. Rook, Kyle A Emmitte, Shaun R. Stauffer, Craig W Lindsley, Jens Meiler, and P. Jeffrey Conn

ACS Chem. Neurosci., **Just Accepted Manuscript** • DOI: 10.1021/cn400225x • Publication Date (Web): 16 Feb 2014

ACS Chemical Neuroscience is published by the American Chemical Society. 1155 Sixteenth Street N.W., Washington, DC 20036

	Chemistry; Meiler, Jens; Vanderbilt University Medical Center, Center for Structural Biology; Vanderbilt University Medical Center, Institute of Chemical Biology; Vanderbilt University Medical Center, Department of Pharmacology; Vanderbilt University Medical Center, Department of Chemistry Conn, P.; Vanderbilt University Medical Center, Department of Pharmacology; Vanderbilt University Medical Center, Center for Neuroscience Drug Discovery

Title: Identification of specific ligand-receptor interactions that govern binding and cooperativity of diverse modulators to a common metabotropic glutamate receptor 5 allosteric site

Karen J. Gregory[1, 2, 3#], Elizabeth D. Nguyen[4#], Chrysa Malosh[1, 2], Jeffrey L. Mendenhall[5], Jessica Z. Zic[1,2], Brittney S. Bates[1, 2], Meredith J. Noetzel[1, 2], Emma F. Squire[1, 2], Eric M. Turner[1, 2], Jerri M. Rook[1,2], Kyle A. Emmitte[1, 2, 5], Shaun R. Stauffer[1, 2, 5], Craig W. Lindsley[1, 2,5], Jens Meiler[1, 4, 5,6]* and P. Jeffrey Conn[1, 2]*.

[1] Department of Pharmacology, Vanderbilt University Medical Center, Nashville, TN, USA.

[2] Vanderbilt Center for Neuroscience Drug Discovery, Vanderbilt University Medical Center, Nashville, TN, USA.

[3] Drug Discovery Biology, Monash Institute of Pharmaceutical Sciences, Monash University, Parkville, VIC, Australia.

[4] Center for Structural Biology, Vanderbilt University Medical Center, Nashville, TN, USA.

[5] Department of Chemistry, Vanderbilt University Medical Center, Nashville, TN, USA.

[6] Institute for Chemical Biology, Vanderbilt University Medical Center, Nashville, TN, USA.

[#] these authors contributed equally to this work.

* *To whom correspondence should be addressed: jens.meiler@vanderbilt.edu; jeff.conn@vanderbilt.edu*

Abstract

A common metabotropic glutamate receptor 5 ($mGlu_5$) allosteric site is known to accommodate diverse chemotypes. However, the structural relationship between compounds from different scaffolds and $mGlu_5$ is not well understood. In an effort to better understand the molecular determinants that govern allosteric modulator interactions with $mGlu_5$ we employed a combination of site-directed mutagenesis and computational modeling. With few exceptions, six residues (P654, Y658, T780, W784, S808 and A809) were identified as key affinity determinants across all seven allosteric modulator scaffolds. To improve our interpretation of how diverse allosteric modulators occupy the common allosteric site, we sampled the wealth of $mGlu_5$ structure-activity relationship (SAR) data available by docking 60 ligands (actives and inactives) representing seven chemical scaffolds into our $mGlu_5$ comparative model. To spatially and chemically compare binding modes of ligands from diverse scaffolds, the ChargeRMSD measure was developed. We found a common binding mode for the modulators that placed the long axes of the ligands parallel to the transmembrane helices 3 and 7. W784 in TM6 was not only identified as a key NAM cooperativity determinant across multiple scaffolds, but also caused a NAM to PAM switch for two different scaffolds. Moreover, a single point mutation in TM5, G747V, altered the architecture of the common allosteric site such that 4-nitro-*N*-(1,3-diphenyl-1*H*-pyrazol-5-yl)benzamide (VU29) was non-competitive with the common allosteric site. Our findings highlight the subtleties of allosteric modulator binding to $mGlu_5$ and demonstrate the utility in incorporating SAR information to strengthen the interpretation and analyses of docking and mutational data.

Keywords: mutagenesis, metabotropic glutamate receptor 5, structure-activity relationships, operational model, cooperativity, affinity

Introduction

Glutamate, a primary excitatory neurotransmitter within the mammalian central nervous system, mediates its effects via interactions with ionotropic and metabotropic glutamate receptors (*1*). The metabotropic glutamate receptors (mGlu) are a family of eight subtypes ($mGlu_1$-$mGlu_8$) that belong to family C seven transmembrane-spanning G protein-coupled receptors (7TMR). Based on physiology and pathophysiology, metabotropic glutamate receptor subtype 5 ($mGlu_5$) is an attractive therapeutic target for a range of CNS-related disorders including: cognitive disorders, Fragile X Syndrome, anxiety, depression, Parkinson's disease and schizophrenia among others (*2*).

However, selective targeting of $mGlu_5$ has been a challenge as the glutamate-binding (orthosteric) site is highly conserved across all mGlu subtypes. An alternative and highly successful approach is to target allosteric binding sites that are topographically distinct from the orthosteric site (*3, 4*). The first of these so-called, allosteric modulators, to be discovered for $mGlu_5$ was MPEP (*5, 6*). Allosteric modulators have the potential to enhance (positive allosteric modulators or PAMs) or inhibit (negative allosteric modulators or NAMs) the response to glutamate. A third category, silent (or neutral) allosteric modulators (SAMs) occupy allosteric sites but do not alter receptor activity. The magnitude and direction of allosteric modulation is referred to as cooperativity. In addition, multiple mGlu PAM scaffolds also exhibit intrinsic agonist activity in the absence of glutamate and such compounds are referred to as ago-PAMs (*7*). At the ligand-receptor interaction level, what governs modulator affinity versus cooperativity and/or agonism remains to be fully appreciated.

In addition to increased subtype selectivity, allosteric modulators offer multiple theoretical advantages over competitive orthosteric ligands. Modulators that are quiescent in the absence of the endogenous agonist have the potential for spatial and temporal modulation of receptor function and therefore are able to 'fine-tune' receptor activity when the endogenous agonist is present. This is a particularly attractive feature for a CNS target as 'fine-tuning' neurotransmission may yield a better therapeutic outcome than sustained activation or blockade. Moreover, the cooperativity between the two sites is saturable, such that allosteric modulators reach a 'ceiling level' to their effect that could provide a larger therapeutic index.

Efforts to develop $mGlu_5$ allosteric modulators have been particularly successful. Numerous chemotypes have been disclosed that encompass the full range of modulator pharmacology, including weak and full NAMs, ago-PAMs, pure PAMs and SAMs. Despite this success, structure-activity relationships (SAR) for mGlu modulators are often difficult to interpret. Often, minimal changes to a molecule will translate to a complete loss of activity (*8*). Furthermore, multiple mGlu chemotypes display "molecular switches' where a PAM or SAM arises from a NAM scaffold and vice versa (*9*). These molecular switches have been noted in numerous $mGlu_5$ modulator chemotypes (*10-15*) and can also give rise to unanticipated changes in subtype selectivity (*16*). This complexity in modulator SAR continues to be a challenge for drug discovery. It is important to note that the vast majority of discovery programs rely upon potency data alone, such that it remains to be determined whether the 'flat' or 'steep' SAR and 'molecular switches' may be attributed to changes in modulator affinity and/or cooperativity. Thus, there is a pressing need for a better understanding at both the ligand and receptor level as to what contributes to affinity versus cooperativity.

We sought to explore the structural determinants within $mGlu_5$ required for ligand binding to the common allosteric site, within and across different chemical scaffolds. We employed a suite of single point mutations that are either known or predicted to contribute to the common allosteric site (*17-23*). Six key residues (P654, Y658, T780, W784, S808 and A809) were consistently implicated as affinity determinants for diverse PAMs and NAMs, validating that these seven chemotypes interact with a common binding pocket. However, a number of mutations showed differential effects on affinity and/or cooperativity between different scaffolds. To facilitate interpretation of mutagenic data and delineation of affinity versus cooperativity determinants, 9-10 analogs from each series, including active and inactive compounds, were docked into our comparative model of $mGlu_5$. Building upon the previous observation that W784 was a crucial for MPEP cooperativity, we found that W784A caused a NAM to PAM switch for two different NAM scaffolds. Herein, we've taken advantage of the plethora of $mGlu_5$ SAR data to facilitate rationalization of binding pose selection for compounds docked to a $mGlu_5$ comparative model, strengthening hypotheses regarding the specific ligand-receptor contacts that dictate the binding and

cooperativity of diverse allosteric modulators. The results highlight the subtleties of small molecule binding within the $mGlu_5$ 7TM domain.

Results and Discussion

Probing determinants of allosteric modulation within the common allosteric site

A common allosteric site of $mGlu_5$, originally characterized as a site for the $mGlu_5$ NAM MPEP (*5, 22, 24*), recognizes multiple chemotypes that encompass the full array of allosteric ligand pharmacology including ago-PAMs, pure PAMs, NAMs and SAMs (*3, 4, 10, 13*). Developing a deeper understanding of how allosteric ligands occupy the pocket and transmit their cooperativity will be important for interpreting the complexities inherent in allosteric modulator SAR. In addition, these insights will enrich our understanding of how class C GPCRs function and inform drug discovery efforts for this receptor class. To achieve this, we assessed representatives from seven allosteric modulator chemical scaffolds across a panel of single point mutations hypothesized to contribute to a common allosteric site in $mGlu_5$ (*17-22*). Building on our previous findings with MPEP, we assessed M-5MPEP, a related compound with lower affinity and cooperativity, in addition to three full NAMs: VU0285683, VU0366058 and VU0409106; two partial NAMs: VU0366248 and VU0366249; and two PAMs: VU29 and DPFE. Mutations were screened for the effect of a single, sub-maximal modulator concentration (based on wildtype) to alter the glutamate concentration response curve for intracellular Ca^{2+} mobilization (Supplementary Fig. 1). Mutations that significantly altered modulation in the single concentration screen (Supplementary Fig. 2) were assessed using the operational model of allosterism to determine modulator affinity and cooperativity estimates (*25*). As expected for ligands interacting with a common pocket, many similarities were seen with respect to the impact of mutations on modulator affinity (Fig. 1).

<Figure 1>

Identification of NAM-receptor interactions that govern affinity

With few exceptions, P654, Y658, T780, W784, S808 and A809 were implicated as affinity determinants; in good agreement with previous studies (*18-22*). To facilitate interpretation of mutagenesis data, representatives from each NAM chemotype (VU0366248, VU0409106, VU0285683, VU0366058) were docked into our comparative model of the $mGlu_5$ 7TM domains in comparison with the reference

prototypical NAM, MPEP (*17*). In our previous efforts investigating the binding modes of MPEP and acetylenic PAMs we found it difficult to computationally differentiate binding poses of these relatively linear ligands (*17*). Therefore, we took advantage of the wealth of available SAR data for these different chemotypes to strengthen interpretations of putative binding poses with the aim to define the specific ligand-receptor interactions governing affinity and cooperativity. For $mGlu_5$ NAMs, with the exception of VU0285683 where very few analogs have been reported (*12*), we identified the best-in-class and minimally active pharmacophore for each scaffold (Table 1, Supplementary Fig. 3) and docked 9-12 analogs (Fig.2), including three inactive (or very low potency) compounds. To compare common binding modes across different ligands within the same scaffold, a new measure was introduced called ChargeRMSD. This measure allowed comparison of ligand conformations by their spatial similarly and conservation of chemical properties, such that conserved ligand SAR becomes a key factor to determine binding modes (Supplementary Materials and Supplementary Fig 4). In comparison, traditional RMSD calculations only capture structural similarities between common atoms of ligands.

<Figure 2>

Direct interactions with S808 may mediate binding of NAMs with cyano substitutions on ring B

All five 4-aryl-5-cyanopyrimidine active ligands converged to two possible binding poses, one with the cyano group buried (Fig. 2a), the other with the cyano group pointing towards extracellular space (Fig. 2b). The 5-cyano is crucial for potency in this series (*26*) and if buried within the pocket, a hydrogen bond with T780 is predicted (Fig. 2a). However, VU0366058 affinity was unaffected by T780A, favoring the cluster with 5-cyano pointing up (Fig. 2b). A cyano group is also a key feature of the *N*-aryl benzamide NAMs (represented by VU0366248); substitution of ring B with 3-cyano yields the most potent ligands (*27*). We postulate that the cyano group, or possibly the 5-fluoro, interacts with S808 (Fig. 2c); consistent with decreased *N*-aryl benzamide (VU0366248 and VU0366249) affinity at S808A while S808T increases affinity. Moreover, T780A had differential effects on the affinity of VU0366248 and VU0366249; these compounds only differ with respect to the position of fluoro substituent on ring A. Interestingly, S808A reduced M-5MPEP affinity by 260 fold versus only 40 fold for MPEP. We

previously hypothesized that S808 may be crucial for initial receptor recognition by MPEP via the pyridine ring. Indeed, the position of the nitrogen in the pyridine ring is crucial for NAM activity (*28*). Docking of acetylene NAMs with methoxy substituents (1C, 1F, 1G) on ring B (Fig. 2g) revealed the methoxy groups coordinated in close proximity to S808. Thus, the increased sensitivity of M-5MPEP to S808A may be related to the 2-methoxy group and/or the pyridine ring interacting with S808. Furthermore, docking of the sub-nanomolar potency analog (1A) that contains a cyano substitution on ring B suggested a potential hydrogen bond with S808 (Fig. 2h). Inactive compounds in both the 4-aryl-5-cyanopyrimidine and *N*-aryl benzamide series docked with the cyano group buried in the pocket (Supplementary Fig. 5). VU0366058 and VU0285683 cooperativity was reduced at S808T and S808A, where these compounds could no longer abolish glutamate activity; however, MPEP and VU0409106 retained full blockade (Table 3). Conversely, VU0366248 and VU0366249, both weak (or partial) NAMs at the wildtype receptor fully blocked glutamate activation of S808T, suggestive of increased negative cooperativity. Importantly, all four NAMs that show altered cooperativity contain a cyano group. These data lend additional support to diverse NAMs binding with ring B higher in the pocket and, where present, a cyano group directly interacting with S808.

Hydrophobic residue cluster in TM5/6 may limit substitution on ring B of NAMs

The most potent/highest affinity *N*-aryl benzamides, for e.g. 2A and 2B, have an additional phenyl substitution on ring B (*29*). Examination of the putative binding pose reveals engagement of cluster of hydrophobic residues in TM5 and 6 (V739, L743, F787 and Y791); and potentially a polar interaction between the 4-fluoro of 2A and Y791. The result is a markedly different binding mode compared to reference compound VU0366248 (Fig. 2d); whereas analogs with a pyridine ring A (2D and 2G) align closer to the VU0366248 cluster. Furthermore, F787A and Y791A increased VU0366058 affinity by 13 and ~2.6 fold respectively (Y791A in supp table); this may be attributed to removal of steric constraints freeing up space in the pocket to accommodate the fluoro-phenyl substituent. These data lend even further support for the putative binding mode with 5-cyano pointing up (Fig. 2b). Bulky substitutions of this

phenyl and polar substitutions were not well tolerated (*26*); inactive compounds in the aryl ether NAM series introduce bulk (e.g. 5L) or polarity (e.g. 5J and 5K) onto ring B (Supplementary Fig. 5) (*30*). Furthermore, analogs of MPEP with a phenyl substitution on ring B (e.g. 1D in Fig 2h) may engage with this hydrophobic cluster; although if ring B is buried, π-π stacking may occur between Y658 and the ligand. Docking of inactive MPEP analogs (Supplementary Fig. 5) revealed that substantial re-orientation of binding pocket residues was required to accommodate the large substitutions of ring B (F787 for 1I and R647 for 1J). Collectively, these data are commensurate with the cluster of hydrophobic residues in TM5/6 having the potential to contribute to high affinity binding, but also limiting the size and polar nature of substitution on ring B of NAMs.

Surprisingly, the O-linked heteroaryl group of the aryl ether benzamide NAMs docked deeper into the binding pocket, rather than interacting with the TM5/6 hydrophobic cluster. This binding pose is favored due to multiple polar interactions predicted between the pyrimidine and backbone of TM7 residues and S657 and T780 side chains (Fig. 2e). From the single concentration screen, S657A and S657C had no effect on modulation by VU0409106 (Supplementary Fig. 5); however, T780A reduced affinity ~10 fold. These data suggest that interactions with T780 and possibly TM7 are more crucial for high affinity binding of VU0409106 and analogs thereof. Further, for the most potent compounds in this series, chloro or fluoro substituents on benzamide ring A are located in the base of the pocket surrounded by W784, T780 and Y658, commensurate with the impact of mutations on VU0409106 affinity (Fig. 1). The minimally active compounds (5H and 5I) lack a substituent in this position, which may account for their drop in potency; whereas methoxy substitution (5G) requires movement of Y658 to occupy the same relative pocket (Fig. 2f).

Amide containing NAMs are sensitive to N746A.

Interestingly, N746A significantly reduced *N*-aryl benzamide affinity (20 fold for VU0366248 and greater than 10 fold for VU0366249) and VU0409106 affinity (15 fold). Reduced affinity was also observed for

VU0285683 (~5 fold) although this did not reach significance. No direct interactions are predicted between these four NAMs and N746. Thus, these effects may be due to indirect changes in the pocket conformation that amide-containing ligands (or those with an oxadiazole replacement) are more sensitive to; such that N746 is important for the overall structure of the binding pocket rather than forming a direct ligand contact.

Determinants of N-aryl piperazine PAM binding

Previously we had examined the interactions of acetylenic PAMs within the common allosteric site of $mGlu_5$ (*17*); it was of interest whether or not PAMs from alternate scaffolds would share affinity and cooperativity determinants. On the whole, the *N*-aryl piperazines are low affinity, cooperativity driven PAMs. Despite this limitation, three compounds from this series are efficacious *in vivo* (*15, 31, 32*). Consistent with interactions within the common allosteric site, P654S, Y658V, T780A, W784A, A809G and A809V decreased affinity of DPFE (6-70 fold). In contrast to all other modulators tested to date, DPFE was unaffected by P654F (Fig 3a). This may be attributable to increased flexibility of this compound allowing binding despite the introduction of a bulky hydrophobic group. Docking results suggest a conserved and relatively linear binding mode, with ring C oriented to the top of the pocket in the vicinity of the TM5/6 hydrophobic cluster and ring A buried; the carbonyl linker may participate in hydrogen bonds with TM7 residues (Fig. 3a). The cyano groups at opposite ends of compounds 6B and 6C are in close proximity to T780 and S808 respectively. In support of this binding mode, we found that compound 6B (VU0364289) was sensitive to the S808A mutation (Supplementary Fig. 7). This pose places the fluoro-phenyl of DPFE in close proximity to T780; Ala substitution of this residue had the most marked effect on DPFE affinity (70 fold; Fig. 3a). Three additional point mutations had unique effects on DPFE: P742S decreased affinity (26 fold), L743V increased affinity (16 fold) and V788A increased affinity (14 fold); affinity increases were confirmed with [^{3}H]methoxyPEPy binding assays (Supplementary Fig. 8). Based on the proposed binding mode, these mutations may change the overall binding pocket architecture, in particular, in relation to the TM5/6 hydrophobic cluster and the capacity to

accommodate the polar difluorophenyl of DPFE. Minimally active (Fig. 4b) and inactive compounds (Fig. 4c) in this series adopted a similar pose. In general, inactives lacked a hydrogen bond partner in the linker region to interact with TM7 (e.g. 6G and 6H) or introduced polarity and/or additional bulk to the phenyl ring C that may not accommodated within the TM5/6 hydrophobic cluster (*15, 33*), similar to the observations noted earlier for NAMs.

<Figure 3>

<Figure 4>

Affinity determinants for diphenylpyrazole benzamide PAMs

In contrast to all other modulators, VU29 was unaffected by Y658V and compared with other PAMs had a moderate affinity reduction at T780A (*17*); possibly due to a lack of hydrogen bond partners in ring A (Fig. 3b). This suggests that diphenylpyrazole benzamide PAM activity is driven via interactions higher in the pocket. All diphenylpyrazole benzamide series ligands docked with consistent positions of all three aromatic rings except for 4E (Fig. 4d & 4e). Notably, ring A of VU29 aligns well with the various NAMs; however, neither ring B nor C overlap (Fig. 6). This deviates significantly from that proposed previously based on 3D superimposition of related ligands (*29*). Further, substitution of the benzamide ring (B) is well tolerated (*29, 34, 35*); with polar interactions predicted between residues at the top of TM5/E2 loop (Fig. 4d & 4e). Moreover, benzamide phenyl replacement with a cyclopentane (4I) or addition of two methoxy groups (4J) significantly lowers PAM potency (*36*). Furthermore, docking of inactive compounds showed deviation from actives, for e.g. phenyl ring C replacement with a pyridine that abolishes PAM activity (4H; Fig. 4f). Indeed, pyridyl replacement or substitution of this phenyl is not tolerated (*35*). G747V selectively reduced VU29 affinity (30-fold); therefore we assessed the ability of VU29 to inhibit [^{3}H]methoxyPEPy binding at G747V (Supplementary Fig. 8). VU29 behaved non-competitively, unable to fully displace [^{3}H]methoxyPEPy binding; recent disclosure of potent dimeric MPEP analogs also suggested the common allosteric pocket could accommodate two ligands simultaneously (*20, 37*). Collectively, these data support a global conformation change in the allosteric site architecture in G747V mutation particularly with respect to TM5/6 hydrophobic residues that may

interact with ring C (Fig. 4e). This is an area of the binding pocket that the other modulators tested do not extend into, therefore accounting for the selective effect of this residue on VU29.

W784 is a NAM cooperativity determinant and can engenders a "molecular switch" to PAM

Similar to its effect on MPEP (*17*), W784A reduced cooperativity of the full NAMs VU0366058 and VU0409106 and abolished M-5MPEP cooperativity and/or affinity (Table 3). Interestingly allosteric modulators VU0285683, VU0366248 and VU0366249 which all maintain a common 3-cyano-5-fluoro pendant phenyl ring, switched their pharmacology to PAMs (Fig. 5). These data beg the question: What is different about how the W784A receptor interacts with VU0366248 and VU0285683 that allows this dramatic switch? W784 is equivalent to Trp of the CWxP motif in class A 7TMRs that is involved receptor activation (*38*). Small increases in positive cooperativity of some, but not all, acetylene PAMs were noted at W784A previously (*17, 23*) while VU29 and DPFE cooperativities were unaffected (Fig. 3c & d) by W784A. Importantly, this mutation does not increase the efficacy of glutamate (*17*), nor do NAMs show inverse agonism indicative of constitutive activity. This differential effect of W784A on the cooperativity of different NAM and PAM scaffolds is indicative of multiple inactive and active 7TM states being engendered by allosteric modulators, such that this pharmacological mode switch relates to W784A favoring active states that are stabilized by certain modulators. In the case of NAMs VU0366248, VU0366249, and VU0285683 it's conceivable that these modulators have a limited mechanism of action on the molecular level, involving an alternative direct hydrogen bond with W784 with the common cyano moiety that is critical for stabilizing an *inactive* form of the receptor. In the absence of this interaction these modulators elicit moderate positive coooperativity with glutamate (Fig. 6, β: ~1.9-2.3). In contrast, VU0366058 and VU0409106, which do retain similar hydrogen bond accepting groups (e.g. cyano and thiazole, VU0366058 and VU0409106, respectively), may be envisioned as having additional interactions with the receptor that contribute to the negative cooperativity that is retained at the W784A mutant. Consistent with this notion, VU0366058 and VU0409106 are structurally more complex with a greater number of rotatable bonds (3-4 vs. 2 RotB) and hydrogen bond acceptors (6 vs. 4); thus these compounds may be able to adopt multiple positions and/or conformations within the binding pocket to retain their

negative cooperativity. In addition, all three weak NAMs (M-5MPEP, VU0366248 and VU0366249) had reduced cooperativity at P654S and increased negative cooperativity at S657A. Together, these data suggest that 1) TM6, and W784 in particular, are crucial for adoption of active receptor states of family C 7TMRs and that 2) these differential effects on cooperativity provide evidence for stabilization of different inactive receptor conformations by individual chemotypes.

<Figure 5>

<Figure 6>

PAM cooperativity determinants within the common allosteric site

Pharmacological mode switches at T780A, F787A or S808A have been observed for certain acetylene PAMs and DFB (*17, 21, 23*) and their cooperativity with glutamate; neither VU29 nor DPFE showed mode switches at any of the mutations tested. However, both P742S and Y791A increased positive cooperativity, with increases also noted for VU29 at L743V and T780A (Fig. 3c & d). Interestingly, Y791A had very low responsiveness to glutamate prohibiting functional assessment of NAMs; however, this could be restored with PAMs (Fig. 3). Collectively, the changes observed for modulator cooperativity highlight the importance of TM3, 5, 6 and 7 in the transmission of cooperativity by both negative and positive $mGlu_5$ allosteric modulators and infer a role for these TMs in the transition of the 7TM region from inactive to active states.

<Figure 7>

Docking PAMs into an inactive template

An important question in homology modeling GPCRs in complex with PAMs is whether a GPCR template in an 'active' state must be used. The critical question is if there is a systematic difference in the position of the upper transmembrane helices between 'active' and 'inactive' templates that might play a role when docking into such a distant sequence homologue? To answer this question we computed pairwise RMSDs between 'active' and 'inactive' structures using the structured-based alignment tool MAMMOTH (3.1±0.5 Å RMSD) (*39*). This value is not significantly higher than the average pairwise RMSD between two inactive structures (2.9±0.6) or two active structures (2.8±0.6). We attribute this

possibly surprising finding to several aspects: A) sequence similarity between GPCRs is so low that structural changes induced by a different sequence are larger than structural changes induced by activation, at least in the upper half of the trans-membrane spanning regions. B) One can also argue that many of the 'active' conformations might not be fully active as no G protein was bound. We conclude that there is no advantage in using an 'active' template when modeling such distant homologues as the structural changes between template and target will be much larger than changes induced by activation. The Rosetta comparative modeling methods are unique in that the backbone template applied to the comparative model is only used to determine the initial placement in transmembrane helices. In the subsequent energy minimization steps, the backbone template is perturb on average 6-8 Å RMSD (*40*). In particular, the binding pocket is perturbed on average 2-4 Å RMSD. Additionally, the flexible docking methods are able to capture the different binding modes of active (Fig. 2 & Fig. 4) versus inactive ligands (Supplementary Fig. 5). In experiments analyzing the accuracy of Rosetta's ligand docking methods when applied to comparative models, Rosetta sampled ligand binding modes within 2.5Å of the binding mode from the crystal structure for 14 7TMRs (*40*). In addition to our analysis, Tautermann and Pautsch examined the binding sites of active and inactive β2-adrenergic receptor (*41*). They show that the binding site is very similar between the inactive and active states and conclude that both – 'active' and 'inactive' state structures – should be considered as templates (*41*). Previous modeling studies with the inactive structure predicted the binding mode of an agonist that overlapped well with that seen in the agonist-bound crystal structure.

Molck and colleagues recently proposed that the binding pocket within the 7TM domains was divided into two by W784, yielding two distinct binding poses for MPEP (*20*). In our model, employment of flexible docking methodology allows rotation of W784 out of the binding pocket. The binding poses determined by computational docking presented herein were filtered by available SAR and mutagenesis information. This ensures that the final pose selected for each scaffold is within interaction distance to the residues implicated by mutagenesis (Fig. 6). Low potency, or inactive, compounds from available SAR were selected that retain some activity to avoid the potential confound of neutral allosteric ligands, i.e.

allosteric ligands that occupy the binding pocket but do not modulate receptor activity. Thus these "inactive" ligands were assumed to be the result of low compatibility with the binding pocket. It is conceivable that inactive compounds may be the result of simply being unable to enter the binding pocket. Currently, for family C 7TMRs there is a lack of appreciation of how allosteric modulators access the transmembrane domains. Lipophilic compounds may enter the pocket via the lipid bilayer or from the top of the pocket opening to extracellular space. In the absence of a family C 7TMR crystal structure these models are not expected to provide high-resolution predictions. However, coupling of mutagenesis-based studies with comparative modeling of 7TMR's has provided powerful tools to study drug-receptor interactions for receptors where crystal structures are unavailable. We anticipate that employment of such a strategy would be operative at other receptors where crystal structures are not available. By applying an operational model of allosterism to quantify the impact of mutations on modulator pharmacology we have leant further power to these analyses, differentiating between effects on affinity versus cooperativity. We identified a single point mutation (W784A) that engendered a molecular switch in NAM pharmacology for two different scaffolds, providing additional insight from the protein perspective as to the propensity of $mGlu_5$ modulator SAR to display molecular switches. It is apparent that a deeper understanding of the specific ligand-receptor interactions has the potential to inform modulator design and potentially aid drug discovery efforts for this important CNS target.

Materials and Methods

Materials

Dulbecco's Modified Eagle's Medium (DMEM), fetal bovine serum (FBS) and antibiotics were purchased from Invitrogen (Carlsbad, CA). VU0409106, VU0366058, VU0366248, VU0366249, M-5MPEP, VU29, DPFE and analogs thereof were all synthesized in-house using previously reported methodologies (*13, 15, 26, 30, 31, 34, 42*). Synthesis of compound 6I is reported in the supplementary information. Unless otherwise stated, all other reagents were purchased from Sigma-Aldrich (St. Louis, MO) and were of an analytical grade.

Cell culture

Mutations were introduced into the wild type rat $mGlu_5$ as described previously (*17*). Polyclonal stable HEK293A-$mGlu_5$ mutant cell lines were maintained in complete DMEM supplemented with 10% FBS, 2 mM L-glutamine, 20 mM HEPES, 0.1 mM Non-Essential Amino Acids, 1 mM sodium pyruvate, antibiotic-antimycotic and 500 μg/mL G418 at 37°C in a humidified incubator containing 5% CO_2, 95% O_2.

Intracellular Ca^{2+} mobilization

Prior to assay, HEK293A-rat $mGlu_5$ cells were seeded at 50,000 cells/well in poly-D-lysine coated black-walled, clear bottom 96 well plates in assay medium (DMEM with 10% dialyzed FBS, 20 mM HEPES, 1 mM sodium pyruvate). On the day of assay, the cell permeable Ca^{2+} indicator dye Fluo-4 (Invitrogen, Carlsbad, CA) was used to assay receptor-mediated Ca^{2+} mobilization as described previously (*17, 25*) using a Flexstation II (Molecular Devices, Sunnyvale, CA).

Docking allosteric modulators into the $mGlu_5$ comparative model

A total of 60 ligands were chosen for computational ligand docking (Table 1 and 2). Conformers for each ligand were first generated with MOE (Molecular Operating Environment, Chemical Computing Group, Ontario, Canada) using the MMFF94x force field and Generalized Born implicit solvent model. Ligand conformers were generated, dependent on the number of rotatable bonds (Table 1), using 10,000 iterations of the Low Mode MD method (*43*) with a redundancy cutoff of 0.25 Å. Ligands were ten computationally docked into our comparative model of $mGlu_5$ (*17*) using Rosetta Ligand (*44-46*). Three rounds of iterative docking were performed and analysis within and across different scaffolds was based on a new measure called ChargeRMSD (see Supplementary Material for further detail).

Figure Legends

Figure 1: Allosteric modulator affinity estimates at mutant $mGlu_5$ constructs

Progressive modulator-induced shifts in the glutamate concentration response curve for calcium mobilization were quantified with the operational model of allosterism to estimate affinity for a) VU0285683, b) VU0366058, c) VU0409106, d) VU0366248, e) M-5MPEP, f) VU0366249. Data represent mean±s.e.m of a minimum of three independent experiments, unless indicated otherwise. # denotes mean of two independent determinations; * indicates significantly different to wild type value, $p<0.05$, one-way ANOVA with Dunnet's post-test. n.d. indicates not determined. "No NAM" indicates no inhibition of the glutamate response was observed up to 10 μM of modulator. # denotes key determinant residue identified from mutagenesis. To facilitate understanding of ligand superimposition in subsequent figures aryl rings are denoted as either "A" or "B".

Figure 2: Combining mutagenesis and SAR to understand binding modes of $mGlu_5$ NAMs

Binding modes from the largest clusters for each ligand are shown, docked into the $mGlu_5$ comparative model. Key residues implicated in ligand affinity for each scaffold, in addition to the six residues (P654, Y658, T780, W784, S808 and A809) identified as key determinants across all seven scaffolds are shown in sticks. a & b) 4-aryl-5-cyanopyrimidine NAM docking with 3A in purple, 3B in cyan, 3C (VU0366058) in black, 3D in beige, 3E in green. c & d) Docking of *N*-aryl benzamide NAMs with 2A in purple, 2B in cyan, 2C in beige, 2D in green, 2E (VU0366248) in black, 2F in blue, 2G in pink. e & f) Docking of aryl ether benzamide NAMs with 5A in purple, 5B in cyan, 5C in beige, 5D (VU0409106) in black, 5E in green, 5F in blue, 5G in light pink, 5H in light blue, 5I in light green. g & h) Acetylene NAM docking with 1A in purple, 1B in cyan, 1C in beige, 1D in green, 1E (MPEP) in black, 1F in blue, 1G in pink.

Figure 3: Impact of mutations within the common allosteric site on $mGlu_5$ PAMs

Progressive modulator-induced shifts in the glutamate concentration response curve for calcium mobilization were quantified with the operational model of allosterism to estimate affinity for a) VU29 and b) DPFE as well as cooperativity c) DPFE and d) VU29. VU29 potentiation of glutamate-mediated Ca^{++} mobilization at wild-type (e) and Y791A (f). DPFE potentiation of glutamate-mediated Ca^{++} mobilization at wild-type (g) and Y791A (h). Data represent mean±s.e.m of a minimum of three

independent experiments. * indicates significantly different to wild type value, $p<0.05$, one-way ANOVA with Dunnet's post-test. # denotes key determinant residue identified from mutagenesis.

Figure 4: Combining mutagenesis and SAR to understand binding modes of $mGlu_5$ PAMs.

Binding modes from the largest clusters for each ligand are shown highlighting key residues implicated in ligand affinity for each scaffold in addition to the six residues (P654, Y658, T780, W784, S808 and A809) identified as key affinity determinants across all seven allosteric modulator scaffolds. a-c) Docking of *N*-aryl piperazine PAMs with 6A (DPFE) in black, 6B in purple, 6C in cyan, 6D in beige, 6E in green, 6F in blue, 6G in orange 6H in red and 6I in yellow. d-f) Docking of diphenylpyrazole benzamide PAMs with 4A (VU29) in black, 4B in purple, 4C in cyan, 4D in beige, 4F in green, 4G in pink, 4H in orange, 4I in red and 4J in yellow.

Figure 5: W784A impacts NAM cooperativity and can cause a molecular switch from NAM to PAM.

Glutamate-mediated Ca^{++} mobilization is inhibited by VU0285683 at wild-type (a) and enhanced at W784A (b). VU0366058 completely abolishes glutamate-mediated Ca^{++} mobilization by at wild-type (c) but has decreased negative cooperativity at W784A (d). Glutamate-mediated Ca^{++} mobilization is inhibited by VU0366248 and VU0366249 at wild-type (e, g) and enhanced at W784A (f, h). Data represent mean±s.e.m of a minimum of three independent experiments.

Figure 6: Comparison of modulator scaffolds and relationship to cooperativity at wild-type vs W784A.

NAMs in the top panel show reduced negative cooperativity (or are inactive) at W784A. NAMs in the bottom panel that share a common cyano moiety exhibit a mode switch in cooperativity from NAM to PAM at W784A.

Figure 7: Overlay of top binding modes for diverse allosteric modulator scaffolds

A representative ligand from each scaffold was docked into the $mGlu_5$ comparative model (a). Binding modes from the largest clusters for each ligand are shown and are within interaction distance of key residues identified from mutational experiments labeled and colored purple (b). Colors corresponding to

each ligand are as follows: MPEP is black, VU0285683 is purple, VU0409106 is cyan, VU0366248 is beige, VU0366058 is green, VU29 is blue and DPFE is pink. Positions of aromatic rings "A" and "B" are similar in c) MPEP, VU0285683 and VU0409106 as well as d) MPEP, VU0366248 and VU0366058. e) While ring position is not conserved, linear positioning of MPEP, VU29 and DPFE are similar when interacting with the common allosteric site.

Acknowledgements:

This work is supported by the National Institute of Mental Health [Grant 2R01 MH062646-13]; National Institute of Neurological Disorders and Stroke (NINDS) [Grant 2R01 NS031373-16A2]; National Institute of Drug Abuse [Grant 1R01 DA023947]; and Molecular Libraries Probe Production Centers Network [Grant 5 u54 MH84659-03, 5 u54 MH84659-03S1]. KJG is the recipient of: National Alliance for Research on Schizophrenia and Depression-Maltz Young Investigator Award; American Australian Association Merck Foundation Fellowship; and National Health and Medical Research Council (Australia) Overseas Biomedical Postdoctoral Training Fellowship. EDN is funded by the PhRMA Foundation Paul Calabresi Medical Student Fellowship. MJN is supported by a National Research Service Award from NINDS [Grant F32 NS071746]. Work in the Meiler laboratory is supported through the National Institutes of Health [R01 GM080403, R01 MH090192, R01 GM099842] and the National Science Foundation [Career 0742762]. The authors acknowledge Philine Hietschold for her contribution to initial docking studies.

Supporting Information Available: Supporting information includes general chemistry methods for previously unpublished compounds, additional detail for docking of allosteric modulators and the new clustering method used as well as additional functional and binding datasets to support the conclusions in the text. This information is available free of charge via the Internet at http://pubs.acs.org/.

REFERENCES

1. Niswender, C. M., and Conn, P. J. (2010) Metabotropic glutamate receptors: physiology, pharmacology, and disease, *Annu Rev Pharmacol Toxicol 50*, 295-322.
2. Gregory, K. J., Noetzel, M. J., and Niswender, C. M. (2013) Pharmacology of metabotropic glutamate receptor allosteric modulators: structural basis and therapeutic potential for CNS disorders, *Prog Mol Biol Transl Sci 115*, 61-121.
3. Stauffer, S. R. (2011) Progress toward Positive Allosteric Modulators of the Metabotropic Glutamate Receptor Subtype 5 (mGlu5), *ACS Chem Neurosci 2*, 450-470.
4. Emmitte, K. A. (2011) Recent Advances in the Design and Development of Novel Negative Allosteric Modulators of mGlu5, *ACS Chem Neurosci 2*, 411-432.
5. Gasparini, F., Lingenhohl, K., Stoehr, N., Flor, P. J., Heinrich, M., Vranesic, I., Biollaz, M., Allgeier, H., Heckendorn, R., Urwyler, S., Varney, M. A., Johnson, E. C., Hess, S. D., Rao, S. P., Sacaan, A. I., Santori, E. M., Velicelebi, G., and Kuhn, R. (1999) 2-Methyl-6-(phenylethynyl)-pyridine (MPEP), a potent, selective and systemically active mGlu5 receptor antagonist, *Neuropharmacology 38*, 1493-1503.
6. Varney, M. A., Cosford, N. D., Jachec, C., Rao, S. P., Sacaan, A., Lin, F. F., Bleicher, L., Santori, E. M., Flor, P. J., Allgeier, H., Gasparini, F., Kuhn, R., Hess, S. D., Velicelebi, G., and Johnson, E. C. (1999) SIB-1757 and SIB-1893: selective, noncompetitive antagonists of metabotropic glutamate receptor type 5, *J Pharmacol Exp Ther 290*, 170-181.
7. Noetzel, M. J., Rook, J. M., Vinson, P. N., Cho, H. P., Days, E., Zhou, Y., Rodriguez, A. L., Lavreysen, H., Stauffer, S. R., Niswender, C. M., Xiang, Z., Daniels, J. S., Jones, C. K., Lindsley, C. W., Weaver, C. D., and Conn, P. J. (2012) Functional impact of allosteric agonist activity of selective positive allosteric modulators of metabotropic glutamate receptor subtype 5 in regulating central nervous system function, *Mol Pharmacol 81*, 120-133.
8. Zhao, Z., Wisnoski, D. D., O'Brien, J. A., Lemaire, W., Williams, D. L., Jr., Jacobson, M. A., Wittman, M., Ha, S. N., Schaffhauser, H., Sur, C., Pettibone, D. J., Duggan, M. E., Conn, P. J., Hartman, G. D., and Lindsley, C. W. (2007) Challenges in the development of mGluR5 positive allosteric modulators: the discovery of CPPHA, *Bioorg Med Chem Lett 17*, 1386-1391.
9. Wood, M. R., Hopkins, C. R., Brogan, J. T., Conn, P. J., and Lindsley, C. W. (2011) "Molecular switches" on mGluR allosteric ligands that modulate modes of pharmacology, *Biochemistry 50*, 2403-2410.
10. Hammond, A. S., Rodriguez, A. L., Townsend, S. D., Niswender, C. M., Gregory, K. J., Lindsley, C. W., and Conn, P. J. (2010) Discovery of a Novel Chemical Class of mGlu(5) Allosteric Ligands with Distinct Modes of Pharmacology, *ACS Chem Neurosci 1*, 702-716.
11. Lamb, J. P., Engers, D. W., Niswender, C. M., Rodriguez, A. L., Venable, D. F., Conn, P. J., and Lindsley, C. W. (2011) Discovery of molecular switches within the ADX-47273 mGlu5 PAM scaffold that modulate modes of pharmacology to afford potent mGlu5 NAMs, PAMs and partial antagonists, *Bioorg Med Chem Lett 21*, 2711-2714.
12. Rodriguez, A. L., Grier, M. D., Jones, C. K., Herman, E. J., Kane, A. S., Smith, R. L., Williams, R., Zhou, Y., Marlo, J. E., Days, E. L., Blatt, T. N., Jadhav, S., Menon, U. N., Vinson, P. N., Rook, J. M., Stauffer, S. R., Niswender, C. M., Lindsley, C. W., Weaver, C. D., and Conn, P. J. (2010) Discovery of novel allosteric modulators of metabotropic glutamate receptor subtype 5 reveals chemical and functional diversity and in vivo activity in rat behavioral models of anxiolytic and antipsychotic activity, *Mol Pharmacol 78*, 1105-1123.
13. Rodriguez, A. L., Nong, Y., Sekaran, N. K., Alagille, D., Tamagnan, G. D., and Conn, P. J. (2005) A close structural analog of 2-methyl-6-(phenylethynyl)-pyridine acts as a neutral allosteric site ligand on metabotropic glutamate receptor subtype 5 and blocks the effects of multiple allosteric modulators, *Mol Pharmacol 68*, 1793-1802.

14. Sharma, S., Kedrowski, J., Rook, J. M., Smith, R. L., Jones, C. K., Rodriguez, A. L., Conn, P. J., and Lindsley, C. W. (2009) Discovery of molecular switches that modulate modes of metabotropic glutamate receptor subtype 5 (mGlu5) pharmacology in vitro and in vivo within a series of functionalized, regioisomeric 2- and 5-(phenylethynyl)pyrimidines, *J Med Chem 52*, 4103-4106.
15. Zhou, Y., Manka, J. T., Rodriguez, A. L., Weaver, C. D., Days, E. L., Vinson, P. N., Jadhav, S., Hermann, E. J., Jones, C. K., Conn, P. J., Lindsley, C. W., and Stauffer, S. R. (2010) Discovery of N-Aryl Piperazines as Selective mGluR5 Potentiators with Improved In Vivo Utility, *ACS Med Chem Lett 1*, 433-438.
16. Sheffler, D. J., Wenthur, C. J., Bruner, J. A., Carrington, S. J. S., Vinson, P. N., Gogi, K. K., Blobaum, A. L., Morrison, R. D., Vamos, M., Cosford, N. D. P., Stauffer, S. R., Scott Daniels, J., Niswender, C. M., Jeffrey Conn, P., and Lindsley, C. W. (2012) Development of a novel, CNS-penetrant, metabotropic glutamate receptor 3 (mGlu3) NAM probe (ML289) derived from a closely related mGlu5 PAM, *Bioorg Med Chem Lett 22*, 3921-3925.
17. Gregory, K. J., Nguyen, E. D., Reiff, S. D., Squire, E. F., Stauffer, S. R., Lindsley, C. W., Meiler, J., and Conn, P. J. (2013) Probing the metabotropic glutamate receptor 5 (mGlu(5)) positive allosteric modulator (PAM) binding pocket: discovery of point mutations that engender a "molecular switch" in PAM pharmacology, *Mol Pharmacol 83*, 991-1006.
18. Malherbe, P., Kratochwil, N., Muhlemann, A., Zenner, M.-T., Fischer, C., Stahl, M., Gerber, P. R., Jaeschke, G., and Porter, R. H. P. (2006) Comparison of the binding pockets of two chemically unrelated allosteric antagonists of the mGlu5 receptor and identification of crucial residues involved in the inverse agonism of MPEP, *J Neurochem 98*, 601-615.
19. Malherbe, P., Kratochwil, N., Zenner, M. T., Piussi, J., Diener, C., Kratzeisen, C., Fischer, C., and Porter, R. H. (2003) Mutational analysis and molecular modeling of the binding pocket of the metabotropic glutamate 5 receptor negative modulator 2-methyl-6-(phenylethynyl)-pyridine, *Mol Pharmacol 64*, 823-832.
20. Molck, C., Harpsoe, K., Gloriam, D. E., Clausen, R. P., Madsen, U., Pedersen, L. O., Jimenez, H. N., Nielsen, S. M., Mathiesen, J. M., and Brauner-Osborne, H. (2012) Pharmacological Characterization and Modeling of the Binding Sites of Novel 1,3-bis(pyridinylethynyl)benzenes as Metabotropic Glutamate Receptor 5-selective Negative Allosteric Modulators, *Mol Pharmacol*. *82*, 929-937.
21. Muhlemann, A., Ward, N. A., Kratochwil, N., Diener, C., Fischer, C., Stucki, A., Jaeschke, G., Malherbe, P., and Porter, R. H. (2006) Determination of key amino acids implicated in the actions of allosteric modulation by 3,3'-difluorobenzaldazine on rat mGlu5 receptors, *Eur J Pharmacol 529*, 95-104.
22. Pagano, A., Ruegg, D., Litschig, S., Stoehr, N., Stierlin, C., Heinrich, M., Floersheim, P., Prezeau, L., Carroll, F., Pin, J. P., Cambria, A., Vranesic, I., Flor, P. J., Gasparini, F., and Kuhn, R. (2000) The non-competitive antagonists 2-methyl-6-(phenylethynyl)pyridine and 7-hydroxyiminocyclopropan[b]chromen-1a-carboxylic acid ethyl ester interact with overlapping binding pockets in the transmembrane region of group I metabotropic glutamate receptors, *J Biol Chem 275*, 33750-33758.
23. Turlington, M., Noetzel, M. J., Chun, A., Zhou, Y., Gogliotti, R. D., Nguyen, E. D., Gregory, K. J., Vinson, P. N., Rook, J. M., Gogi, K. K., Xiang, Z., Bridges, T. M., Daniels, J. S., Jones, C., Niswender, C. M., Meiler, J., Conn, P. J., Lindsley, C. W., and Stauffer, S. R. (2013) Exploration of Allosteric Agonism Structure-Activity Relationships within an Acetylene Series of Metabotropic Glutamate Receptor 5 (mGlu5) Positive Allosteric Modulators (PAMs): Discovery of 5-((3-Fluorophenyl)ethynyl)-N-(3-methyloxetan-3-yl)picolinamide (ML254), *J Med Chem 56*, 7976-7996.
24. Cosford, N. D., Roppe, J., Tehrani, L., Schweiger, E. J., Seiders, T. J., Chaudary, A., Rao, S., and Varney, M. A. (2003) [3H]-methoxymethyl-MTEP and [3H]-methoxy-PEPy: potent and selective

radioligands for the metabotropic glutamate subtype 5 (mGlu5) receptor, *Bioorg Med Chem Lett 13*, 351-354.

25. Gregory, K. J., Noetzel, M. J., Rook, J. M., Vinson, P. N., Stauffer, S. R., Rodriguez, A. L., Emmitte, K. A., Zhou, Y., Chun, A. C., Felts, A. S., Chauder, B. A., Lindsley, C. W., Niswender, C. M., and Conn, P. J. (2012) Investigating Metabotorpic Glutamate Receptor 5 Allosteric Modulator Cooperativity, Affinity and Agonism: Enriching Structure-function Studies and Structure-activity Relationships, *Mol Pharmacol*. *82*, 860-875.
26. Mueller, R., Dawson, E. S., Meiler, J., Rodriguez, A. L., Chauder, B. A., Bates, B. S., Felts, A. S., Lamb, J. P., Menon, U. N., Jadhav, S. B., Kane, A. S., Jones, C. K., Gregory, K. J., Niswender, C. M., Conn, P. J., Olsen, C. M., Winder, D. G., Emmitte, K. A., and Lindsley, C. W. (2012) Discovery of 2-(2-Benzoxazoyl amino)-4-Aryl-5-Cyanopyrimidine as Negative Allosteric Modulators (NAMs) of Metabotropic Glutamate Receptor 5 (mGlu5): From an Artificial Neural Network Virtual Screen to an In Vivo Tool Compound, *ChemMedChem 7*, 406-414.
27. Kulkarni, S. S., Zou, M. F., Cao, J., Deschamps, J. R., Rodriguez, A. L., Conn, P. J., and Newman, A. H. (2009) Structure-activity relationships comparing N-(6-methylpyridin-yl)-substituted aryl amides to 2-methyl-6-(substituted-arylethynyl)pyridines or 2-methyl-4-(substituted-arylethynyl)thiazoles as novel metabotropic glutamate receptor subtype 5 antagonists, *J Med Chem 52*, 3563-3575.
28. Alagille, D., Baldwin, R. M., Roth, B. L., Wroblewski, J. T., Grajkowska, E., and Tamagnan, G. D. (2005) Synthesis and receptor assay of aromatic-ethynyl-aromatic derivatives with potent mGluR5 antagonist activity, *Bioorg Med Chem 13*, 197-209.
29. Zou, M. F., Cao, J., Rodriguez, A. L., Conn, P. J., and Newman, A. H. (2011) Design and synthesis of substituted N-(1,3-diphenyl-1H-pyrazol-5-yl)benzamides as positive allosteric modulators of the metabotropic glutamate receptor subtype 5, *Bioorg Med Chem Lett 21*, 2650-2654.
30. Felts, A. S., Rodriguez, A. L., Morrison, R. D., Venable, D. F., Manka, J. T., Bates, B. S., Blobaum, A. L., Byers, F. W., Daniels, J. S., Niswender, C. M., Jones, C. K., Conn, P. J., Lindsley, C. W., and Emmitte, K. A. (2013) Discovery of VU0409106: A negative allosteric modulator of mGlu5 with activity in a mouse model of anxiety, *Bioorg Med Chem Lett*. *23*, 5779-5785.
31. Gregory, K. J., Herman, E. J., Ramsey, A. J., Hammond, A. S., Byun, N. E., Stauffer, S. R., Manka, J. T., Jadhav, S., Bridges, T. M., Weaver, C. D., Niswender, C. M., Steckler, T., Drinkenburg, W. H., Ahnaou, A., Lavreysen, H., Macdonald, G. J., Bartolome, J. M., Mackie, C., Hrupka, B. J., Caron, M. G., Daigle, T. L., Lindsley, C. W., Conn, P. J., and Jones, C. K. (2013) N-aryl piperazine metabotropic glutamate receptor 5 positive allosteric modulators possess efficacy in pre-clinical models of NMDA hypofunction and cognitive enhancement, *J Pharmacol Exp Ther*. *347*, 438-457.
32. Spear, N., Gadient, R. A., Wilkins, D. E., Do, M., Smith, J. S., Zeller, K. L., Schroeder, P., Zhang, M., Arora, J., and Chhajlani, V. (2011) Preclinical profile of a novel metabotropic glutamate receptor 5 positive allosteric modulator, *Eur J Pharmacol 659*, 146-154.
33. Xiong, H., Brugel, T. A., Balestra, M., Brown, D. G., Brush, K. A., Hightower, C., Hinkley, L., Hoesch, V., Kang, J., Koether, G. M., McCauley, J. P., Jr., McLaren, F. M., Panko, L. M., Simpson, T. R., Smith, R. W., Woods, J. M., Brockel, B., Chhajlani, V., Gadient, R. A., Spear, N., Sygowski, L. A., Zhang, M., Arora, J., Breysse, N., Wilson, J. M., Isaac, M., Slassi, A., and King, M. M. (2010) 4-aryl piperazine and piperidine amides as novel mGluR5 positive allosteric modulators, *Bioorg Med Chem Lett 20*, 7381-7384.
34. Chen, Y., Nong, Y., Goudet, C., Hemstapat, K., de Paulis, T., Pin, J. P., and Conn, P. J. (2007) Interaction of novel positive allosteric modulators of metabotropic glutamate receptor 5 with the negative allosteric antagonist site is required for potentiation of receptor responses, *Mol Pharmacol 71*, 1389-1398.

35. de Paulis, T., Hemstapat, K., Chen, Y., Zhang, Y., Saleh, S., Alagille, D., Baldwin, R. M., Tamagnan, G. D., and Conn, P. J. (2006) Substituent effects of N-(1,3-diphenyl-1H-pyrazol-5-yl)benzamides on positive allosteric modulation of the metabotropic glutamate-5 receptor in rat cortical astrocytes, *J Med Chem 49*, 3332-3344.
36. Kinney, G. G., O'Brien, J. A., Lemaire, W., Burno, M., Bickel, D. J., Clements, M. K., Chen, T. B., Wisnoski, D. D., Lindsley, C. W., Tiller, P. R., Smith, S., Jacobson, M. A., Sur, C., Duggan, M. E., Pettibone, D. J., Conn, P. J., and Williams, D. L., Jr. (2005) A novel selective positive allosteric modulator of metabotropic glutamate receptor subtype 5 has in vivo activity and antipsychotic-like effects in rat behavioral models, *J Pharmacol Exp Ther 313*, 199-206.
37. Kaae, B. H., Harpsoe, K., Kvist, T., Mathiesen, J. M., Molck, C., Gloriam, D., Jimenez, H. N., Uberti, M. A., Nielsen, S. M., Nielsen, B., Brauner-Osborne, H., Sauerberg, P., Clausen, R. P., and Madsen, U. (2012) Structure-activity relationships for negative allosteric mGluR5 modulators, *ChemMedChem 7*, 440-451.
38. Deupi, X., and Standfuss, J. (2011) Structural insights into agonist-induced activation of G-protein-coupled receptors, *Curr Opin Struct Biol 21*, 541-551.
39. Ortiz, A. R., Strauss, C. E., and Olmea, O. (2002) MAMMOTH (matching molecular models obtained from theory): an automated method for model comparison, *Protein Sci 11*, 2606-2621.
40. Nguyen, E. D., Norn, C., Frimurer, T. M., and Meiler, J. (2013) Assessment and challenges of ligand docking into comparative models of G-protein coupled receptors, *PLoS One 8*, e67302.
41. Tautermann, C. S., and Pautsch, A. (2011) The Implication of the First Agonist Bound Activated GPCR X-ray Structure on GPCR in Silico Modeling, *ACS Med Chem Lett 2*, 414-418.
42. Felts, A. S., Lindsley, S. R., Lamb, J. P., Rodriguez, A. L., Menon, U. N., Jadhav, S., Jones, C. K., Conn, P. J., Lindsley, C. W., and Emmitte, K. A. (2010) 3-Cyano-5-fluoro-N-arylbenzamides as negative allosteric modulators of mGlu(5): Identification of easily prepared tool compounds with CNS exposure in rats, *Bioorg Med Chem Lett 20*, 4390-4394.
43. Labute, P. (2010) LowModeMD--implicit low-mode velocity filtering applied to conformational search of macrocycles and protein loops, *J Chem Inf Model 50*, 792-800.
44. Davis, I. W., and Baker, D. (2009) RosettaLigand docking with full ligand and receptor flexibility, *J Mol Biol 385*, 381-392.
45. Lemmon, G., and Meiler, J. (2012) Rosetta Ligand docking with flexible XML protocols, *Methods Mol Biol 819*, 143-155.
46. Meiler, J., and Baker, D. (2006) ROSETTALIGAND: protein-small molecule docking with full side-chain flexibility, *Proteins 65*, 538-548.
47. Roppe, J., Smith, N. D., Huang, D., Tehrani, L., Wang, B., Anderson, J., Brodkin, J., Chung, J., Jiang, X., King, C., Munoz, B., Varney, M. A., Prasit, P., and Cosford, N. D. (2004) Discovery of novel heteroarylazoles that are metabotropic glutamate subtype 5 receptor antagonists with anxiolytic activity, *J Med Chem 47*, 4645-4648.
48. Alagille, D., Baldwin, R. M., Roth, B. L., Wroblewski, J. T., Grajkowska, E., and Tamagnan, G. D. (2005) Functionalization at position 3 of the phenyl ring of the potent mGluR5 noncompetitive antagonists MPEP, *Bioorg Med Chem Lett 15*, 945-949.

Table 1 Structure-activity relationships for $mGlu_5$ negative allosteric modulators from four diverse scaffolds chosen for this study. Structures for each compound are found in the Supplementary Information.

Allosteric ligand	ID	Conf[a]	IC_{50} (nM)	Ref
Acetylene NAM (MPEP) series				
3-((6-methylpyridin-2-yl)ethynyl)benzonitrile	1A	76	0.4	(*27*)
2-methyl-4-((6-phenylpyridin-3-yl)ethynyl)thiazole	1B	13	0.5	(*47*)
2-((3-methoxyphenyl)ethynyl)-6-methylpyridine	1C	571	8	(*28*)
2-methyl-6-((5-phenylpyridin-3-yl)ethynyl)pyridine	1D	21	20	(*48*)
2-methyl-6-(phenylethynyl)pyridine	1E	735	9	(*25*)
2-((2,5-dimethoxyphenyl)ethynyl)-6-methylpyridine	1F	7	82	(*28*)
2-((3-methoxyphenyl)ethynyl)-5-methylpyridine	1G	459	114	(*13*)
2-methoxy-6-(phenylethynyl)pyridine	1H	651	1961	(*28*)
methyl 2-(3-((6-methylpyridin-2-yl)ethynyl)phenoxy)acetate	1I	553	2400	(*48*)
3-((6-methylpyridin-2-yl)ethynyl)phenyl 4-methylbenzenesulfonate	1J	82	>10000	(*48*)
N-aryl benzamide NAM (VU0366248) series				
2-cyano-4'-fluoro-*N*-(6-methylpyridin-2-yl)-[1,1'-biphenyl]-4-carboxamide	2A	11	5	(*29*)
2-cyano-*N*-(6-methylpyridin-2-yl)-[1,1'-biphenyl]-4-carboxamide	2B	10	14	(*29*)
N-(3-chlorophenyl)-3-cyano-5-fluorobenzamide	2C	8	45	(*42*)
3-cyano-*N*-(6-ethylpyridin-2-yl)-5-fluorobenzamide	2D	26	59	(*29*)
N-(3-chloro-2-fluorophenyl)-3-cyano-5-fluorobenzamide	2E	8	347	(*42*)
N-(3-chloro-4-fluorophenyl)-3-cyano-5-fluorobenzamide	2F	8	377	(*42*)
3-cyano-*N*-(6-methylpyridin-2-yl)benzamide	2G	10	490	(*29*)
3-cyano-5-fluoro-*N*-phenylbenzamide	2H	4	5440	(*42*)
N-(adamantan-1-yl)-3-cyano-5-fluorobenzamide	2I	12	>10000	(*42*)
4-aryl-5-cyanopyrimidine (VU0366058) series				
2-(benzo[*d*]oxazol-2-ylamino)-4-(2-methoxyphenyl)pyrimidine-5-carbonitrile	3A	8	62	(*26*)
2-(benzo[*d*]oxazol-2-ylamino)-4-phenylpyrimidine-5-carbonitrile	3B	8	89	(*26*)
2-(benzo[*d*]oxazol-2-ylamino)-4-(4-fluorophenyl)pyrimidine-5-carbonitrile	3C	8	91	(*26*)
2-(benzo[*d*]oxazol-2-ylamino)-4-cyclohexylpyrimidine-5-carbonitrile	3D	22	216	(*26*)
2-(benzo[*d*]oxazol-2-ylamino)-4-(4-methoxyphenyl)pyrimidine-5-carbonitrile	3E	16	223	(*26*)
2-(benzo[*d*]oxazol-2-ylamino)-4-(3,5-dimethoxyphenyl)pyrimidine-5-carbonitrile	3F	32	>10000	(*26*)
2-(benzo[*d*]oxazol-2-ylamino)-4-(pyridin-2-yl)pyrimidine-5-carbonitrile	3G	8	>10000	(*26*)
2-(benzo[*d*]oxazol-2-ylamino)-4-(naphthalen-2-yl)pyrimidine-5-carbonitrile	3H	16	>10000	(*26*)
Aryl ether benzamide NAM (VU0409106) series				
3-chloro-5-((5-fluoropyridin-3-yl)oxy)-*N*-(6-methylpyridin-2-yl)benzamide	5A	84	5	(*30*)
3-chloro-*N*-(4-methylthiazol-2-yl)-5-(pyrimidin-5-yloxy)benzamide	5B	42	11	(*30*)
3-chloro-5-((5-cyanopyridin-3-yl)oxy)-*N*-(6-methylpyridin-2-yl)benzamide	5C	87	12	(*30*)
3-fluoro-*N*-(4-methylthiazol-2-yl)-5-(pyrimidin-5-yloxy)benzamide	5D	40	26	(*30*)
3-chloro-*N*-(6-methylpyridin-2-yl)-5-(pyrimidin-5-yloxy)benzamide	5E	42	26	(*30*)
3-chloro-*N*-(6-methoxypyridin-2-yl)-5-(pyrimidin-5-yloxy)benzamide	5F	82	49	(*30*)
N-(5-fluoropyridin-2-yl)-3-methoxy-5-(pyrimidin-5-yloxy)benzamide	5G	89	85	(*30*)
N-(4-methylthiazol-2-yl)-3-(pyrimidin-5-yloxy)benzamide	5H	32	205	(*30*)
N-(pyridin-2-yl)-3-(pyridin-3-yloxy)benzamide	5I	84	844	(*30*)
3-chloro-5-(pyrimidin-5-yloxy)-*N*-(5-(trifluoromethyl)pyridin-2-yl)benzamide	5J	38	>10000	(*30*)
3-chloro-*N*-(3-fluoropyridin-2-yl)-5-(pyrimidin-5-yloxy)benzamide	5K	45	>10000	(*30*)
N-(5-bromo-4-methylthiazol-2-yl)-3-fluoro-5-((2-methylpyrimidin-5-yl)oxy)benzamide	5L	83	>10000	(*30*)

[a] number of conformers computed for each ligand for docking.

Table 2 Structure-activity relationships of $mGlu_5$ positive allosteric modulators from two diverse scaffolds chosen for this study. Structures for each compound are found in the Supplementary Information.

Allosteric ligand	ID	Conf[a]	EC_{50} (nM)	Ref
N-aryl piperazine (DPFE) series				
1-(4-(2,4-difluorophenyl)piperazin-1-yl)-2-((4-fluorobenzyl)oxy)ethanone	6A	144	100	(*31*)
5-((2-(4-(2,4-dichlorophenyl)piperazin-1-yl)-2-oxoethoxy)methyl)thiophene-2-carbonitrile	6B	275	210	(*33*)
2-(4-(2-(benzyloxy)acetyl)piperazin-1-yl)benzonitrile	6C	146	320	(*15*)
1-(4-(2,4-dichlorophenyl)piperazin-1-yl)-4-(pyridin-4-yl)butan-1-one	6D	151	530	(*33*)
2-(benzylthio)-1-(4-(2,4-dichlorophenyl)piperazin-1-yl)ethanone	6E	156	710	(*33*)
1-(4-(2,4-dichlorophenyl)piperazin-1-yl)-2-((pyridin-4-ylmethyl)amino)ethanone	6F	170	850	(*33*)
1-(2-(benzyloxy)ethyl)-4-(2,4-dichlorophenyl)piperazine	6G	410	>25000	(*33*)
1-(4-(2-chloro-4-fluorophenyl)piperidin-1-yl)-2-(pyridin-4-ylmethoxy)ethanethione	6H	131	>10000	(*33*)
2-(4-(2-(cyclopentylmethoxy)acetyl)piperazin-1-yl)benzonitrile	6I	449	>10000	#
Diphenylpyrazolebenzamide (VU29) series				
N-(1,3-diphenyl-1*H*-pyrazol-5-yl)-4-nitrobenzamide	4A	7	9	(*34*)
N-(1,3-diphenyl-1*H*-pyrazol-5-yl)-3,4-dimethylbenzamide	4B	13	17	(*34*)
3-cyano-*N*-(1,3-diphenyl-1*H*-pyrazol-5-yl)benzamide	4C	16	45-77	(*34*)
N-(1,3-diphenyl-1*H*-pyrazol-5-yl)-3-nitrobenzamide	4D	15	39	(*34*)
(*E*)-4-cyano-*N*-(1-(4-cyanobenzoyl)-2,5-diphenyl-1*H*-pyrazol-3(2*H*)-ylidene)benzamide	4E	8	43	(*35*)
N-(1,3-diphenyl-1*H*-pyrazol-5-yl)-4-methoxybenzamide	4F	14	54	(*35*)
N-(1,3-diphenyl-1*H*-pyrazol-5-yl)benzamide	4G	5	175	(*34*)
N-(3-phenyl-1-(pyridin-2-yl)-1*H*-pyrazol-5-yl)benzamide	4H	2	>10000	(*35*)
N-(1,3-diphenyl-1*H*-pyrazol-5-yl)cyclopentanecarboxamide	4I	15	3410	(*35*)
N-(1,3-diphenyl-1*H*-pyrazol-5-yl)-3,4-dimethoxybenzamide	4J	87	3530	(*35*)

[a] the number of conformers sampled for ligand docking.

unpublished observation from (*15*), synthesis reported in supplementary materials.

Table 3: Summary of qualitative and quantitative cooperativity estimates (logβ) for $mGlu_5$ NAMs at mutant constructs. Data are mean±s.e.m of 3-5 independent experiments, unless noted otherwise.

mutant	M-5MPEP	VU0366058	VU0285683	VU0409106	VU0366248	VU0366249
R5-wt	-1.00±0.11	Full NAM	Full NAM	Full NAM	-0.88±0.11	-0.66±0.18
P654F	**Weak NAM**	**No NAM**	**No NAM**	**No NAM**	**No NAM**	**No NAM**
P654S	**-0.37±0.08***	**-0.45±0.08**	**Full NAM**	**Full NAM**	**-0.30±0.09***	**Weak NAM**
S657C	Full NAM	n.d.	n.d.	n.d.	Full NAM	-0.23±0.07
S657A	Full NAM	n.d.	n.d.	n.d.	Full NAM	Full NAM
Y658V	**Weak NAM**	**-0.36 [a]**	**Full NAM**	**-0.75±0.10**	**Full NAM**	**No NAM**
P742S	Full NAM	n.d.	Full NAM	n.d.	n.d.	No NAM
N746A	Full NAM	-0.39±0.15	Full NAM	Full NAM	-1.20±0.08	Weak NAM
G747V	-0.46±0.18	Full NAM	Full NAM	Full NAM	Full NAM	Full NAM
T780A	**-0.56±0.08**	**-0.55±0.06**	**Full NAM**	**-0.82±0.09**	**Full NAM**	**Weak NAM**
W784A	**No NAM**	**-0.50±0.17**	**0.27±0.06**	**-0.43±0.08**	**0.29±0.05***	**0.36±0.06***
F787A	Full NAM	Full NAM	Full NAM	Full NAM	No NAM	No NAM
V788A	-0.72±0.22	Full NAM	Full NAM	Full NAM	Full NAM	Full NAM
F792A	n.d.	n.d.	n.d.	Full NAM	Full NAM	n.d.
S808A	**-0.66±0.11**	**-0.44±0.10**	**-0.59±0.14**	**Full NAM**	**-0.80±0.35**	**No NAM**
S808T	**-0.55±0.19**	**-0.39±0.09**	**-0.77±0.19**	**Full NAM**	**Full NAM**	**Full NAM**
A809V	**Full NAM**	**Full NAM**	**Full NAM**	**Full NAM**	**Full NAM**	**No NAM**
A809G	**-0.43 [a]**	**-0.52±0.10**	**Full NAM**	**Full NAM**	**-0.48±0.07**	**No NAM**

* denotes significantly different to wild type, one-way ANOVA, $p<0.05$ Dunnett's post-test.
"Weak NAM" denotes incomplete and non-saturating inhibition of the glutamate response.
"Full NAM" denotes complete abolishment of the glutamate Ca^{2+} mobilization response.
"No NAM" indicates no inhibition of the glutamate response was observed up to 10 μM.
[a] data are mean from two independent experiments.
n.d. denotes not determined
Mutations of the six common determinant residues are highlighted in bold text.

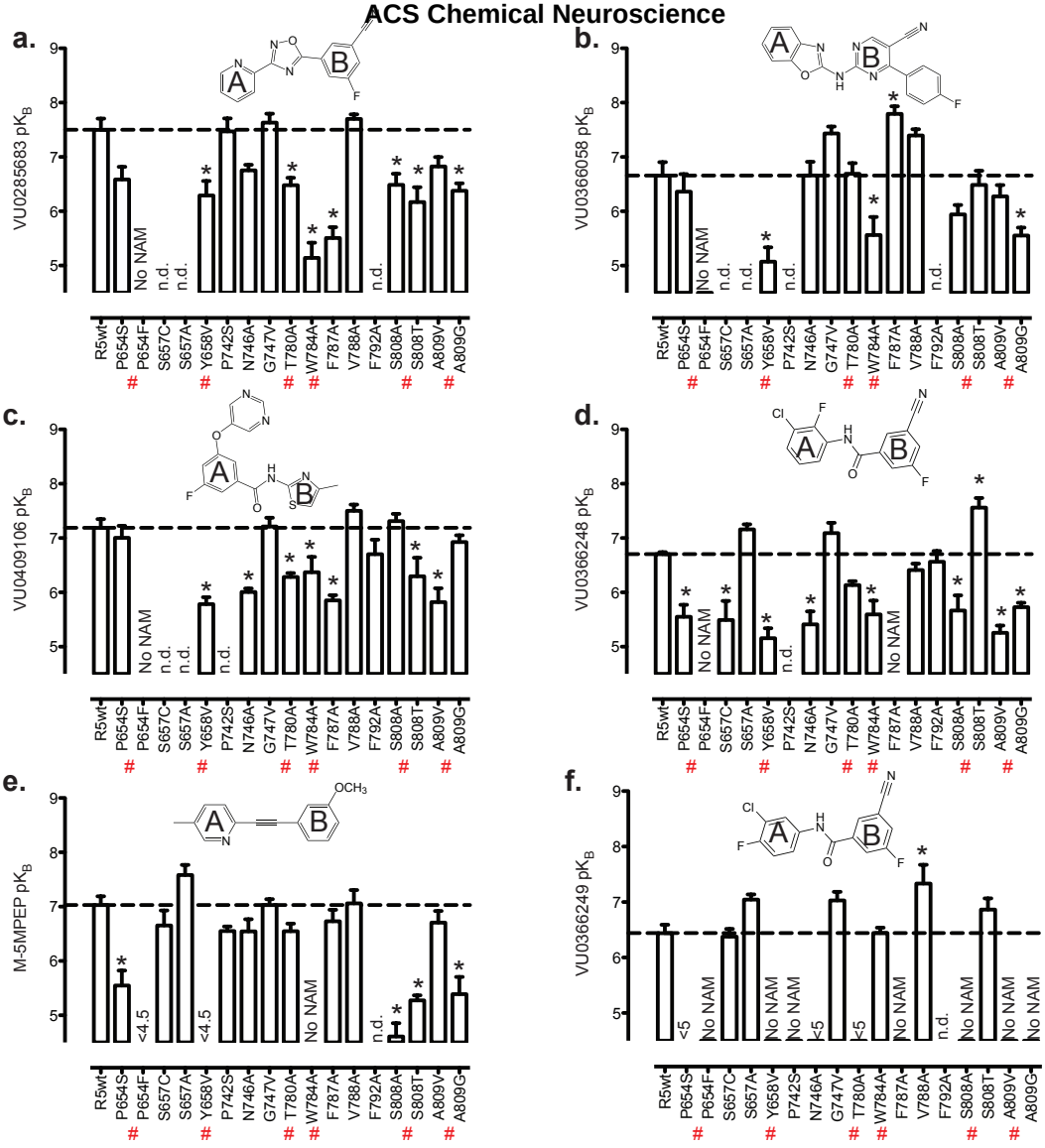
a.
VU0285683 pK$_B$
No NAM
n.d.
b.
VU0366058 pK$_B$
c.
VU0409106 pK$_B$
d.
VU0366248 pK$_B$
e.
M-5MPEP pK$_B$
<4.5
f.
VU0366249 pK$_B$
<5
R5wt
P654S
P654F
S657C
S657A
Y658V
P742S
N746A
G747V
T780A
W784A
F787A
V788A
F792A
S808A
S808T
A809V
A809G

Figure 1

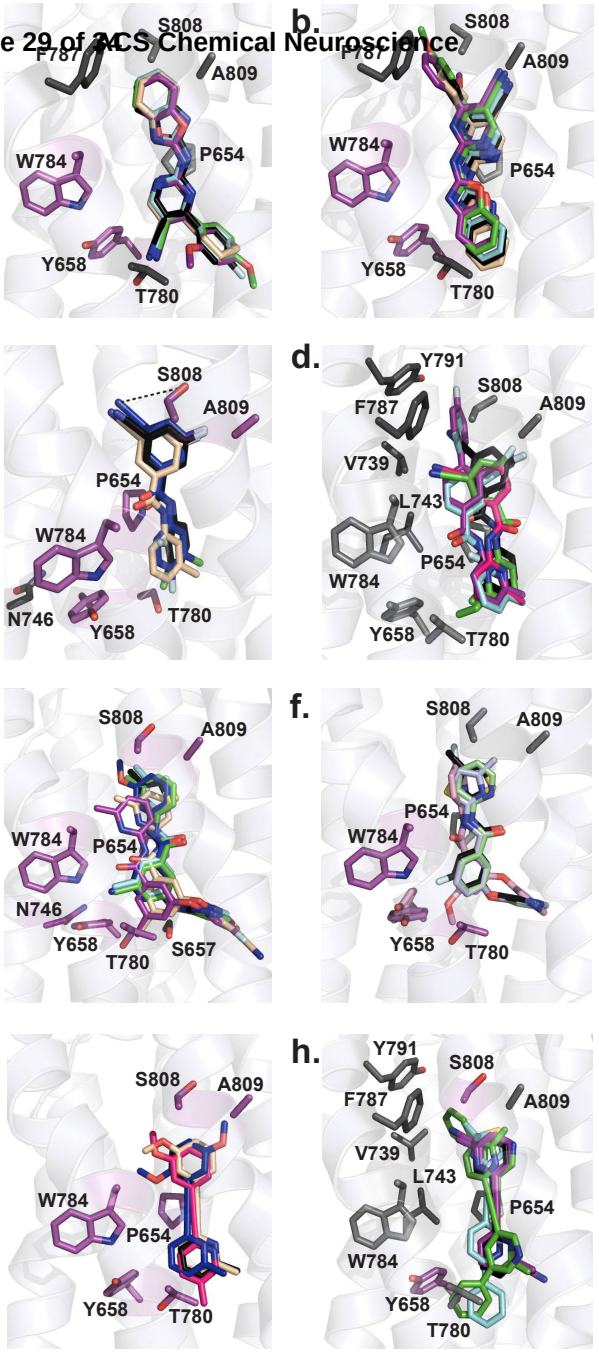

ACS Paragon Plus Environment

Figure 2

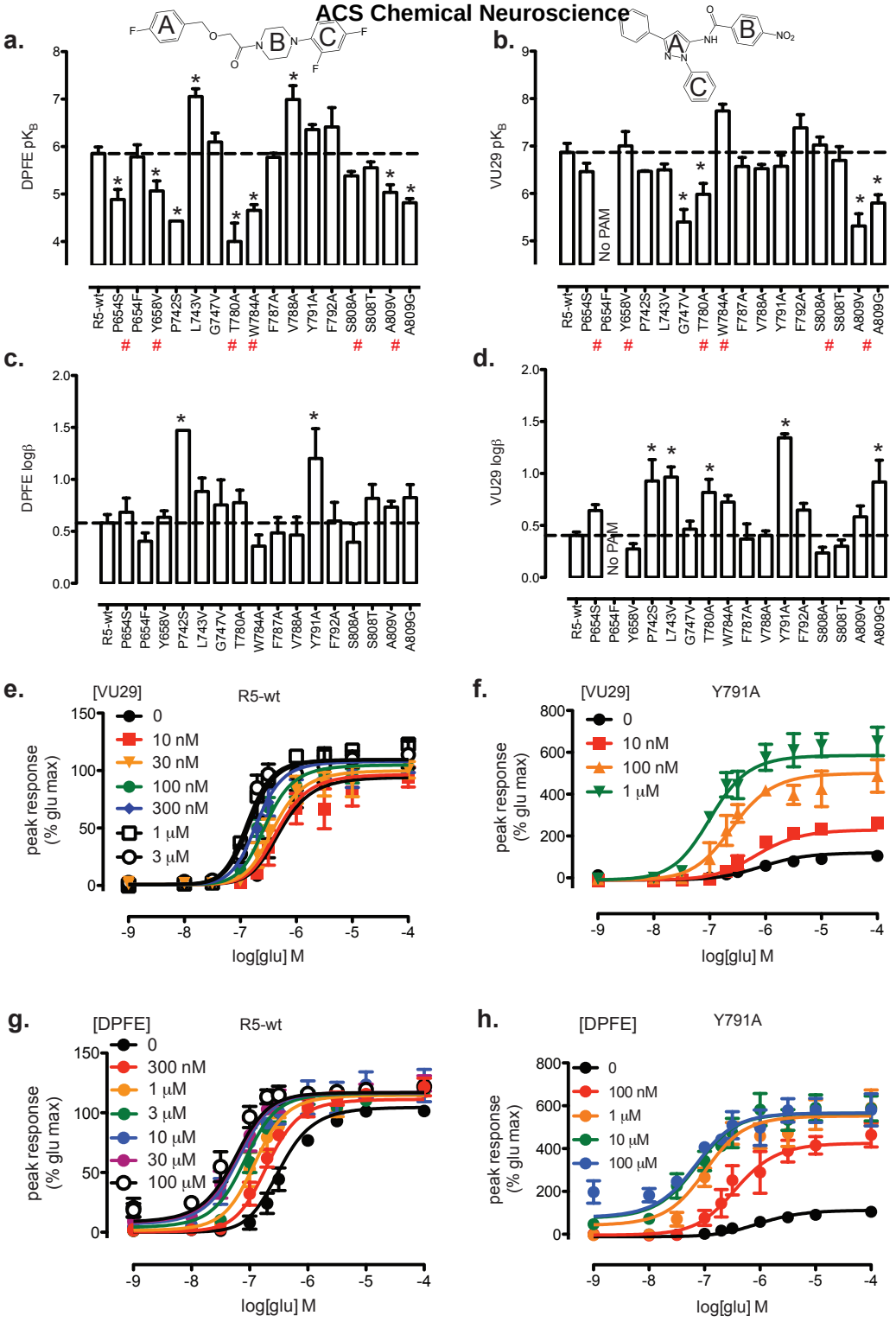
a.
b.
c.
d.
e.
f.
g.
h.
DPFE pKB
VU29 pKB
No PAM
DPFE logβ
VU29 logβ
R5-wt
P654S
P654F
Y658V
P742S
L743V
G747V
T780A
W784A
F787A
V788A
Y791A
F792A
S808A
S808T
A809V
A809G
[VU29]
R5-wt
0
10 nM
30 nM
100 nM
300 nM
1 μM
3 μM
peak response
(% glu max)
log[glu] M
Y791A
[DPFE]
10 μM
30 μM
100 μM

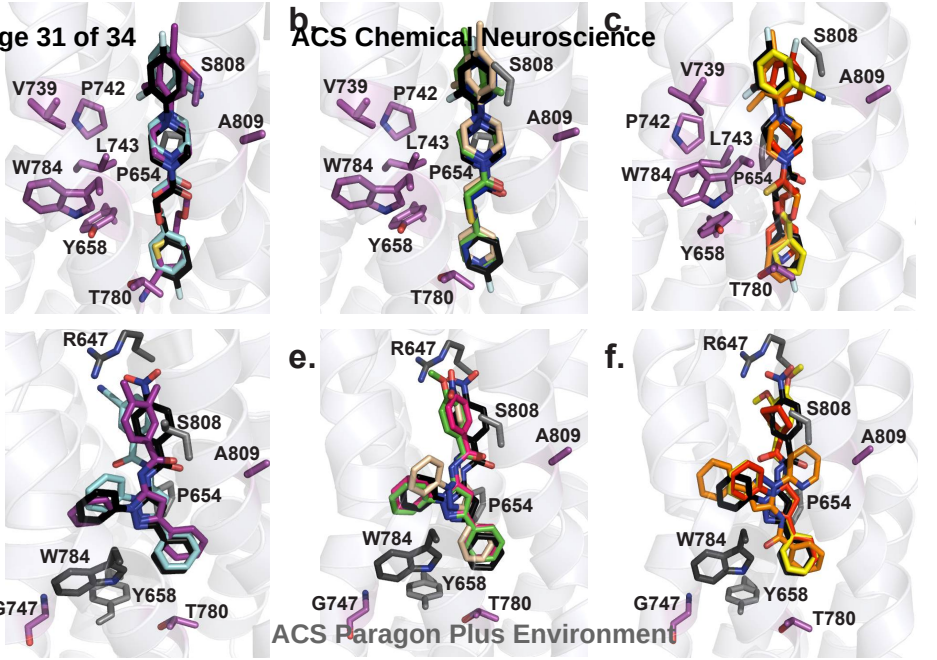
a.
S808
V739
P742
A809
L743
W784
P654
Y658
T780
b.
S808
V739
P742
A809
L743
W784
P654
Y658
T780
c.
S808
V739
A809
P742
L743
W784
P654
Y658
T780
d.
R647
S808
A809
P654
W784
Y658
G747
T780
e.
R647
S808
A809
P654
W784
Y658
G747
T780
f.
R647
S808
A809
P654
W784
Y658
G747
T780
ACS Paragon Plus Environment

Figure 4

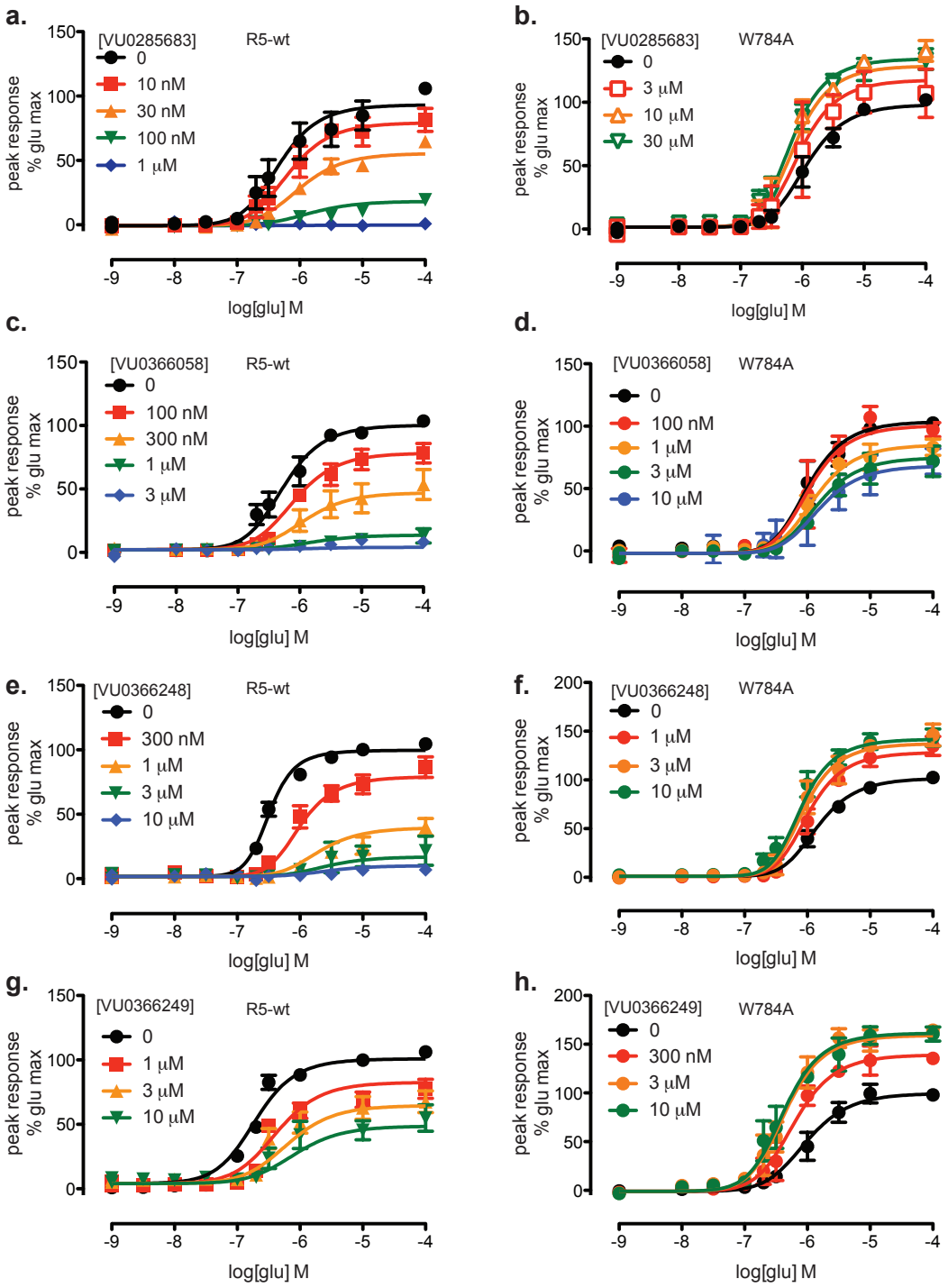
a.
[VU0285683]
R5-wt
0
10 nM
30 nM
100 nM
1 μM
peak response
% glu max
log[glu] M
b.
[VU0285683]
W784A
0
3 μM
10 μM
30 μM
c.
[VU0366058]
R5-wt
0
100 nM
300 nM
1 μM
3 μM
d.
[VU0366058]
W784A
0
100 nM
1 μM
3 μM
10 μM
e.
[VU0366248]
R5-wt
0
300 nM
1 μM
3 μM
10 μM
f.
[VU0366248]
W784A
0
1 μM
3 μM
10 μM
g.
[VU0366249]
R5-wt
0
1 μM
3 μM
10 μM
h.
[VU0366249]
W784A
0
300 nM
3 μM
10 μM

Figure 5

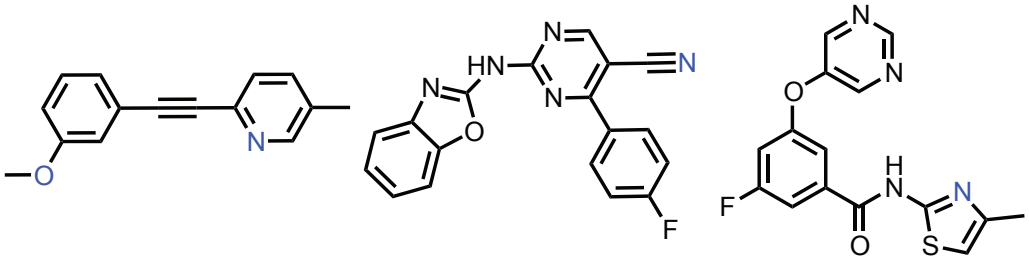

	M-5MPEP	VU0366058	VU0409106
WT	Partial NAM	Full NAM	Full NAM
W784A (β – cooperativity)	inactive	0.31	0.37

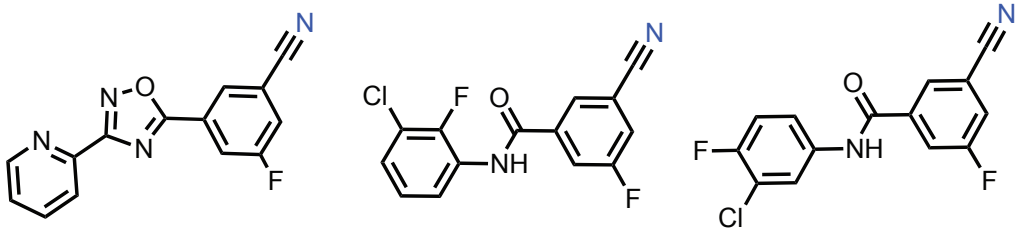

	VU0285683	VU0366248	VU0366249
WT	Full NAM	Partial NAM	Partial NAM
W784A (β – cooperativity)	1.86 (PAM)	1.94 (PAM)	2.29 (PAM)

Figure 6

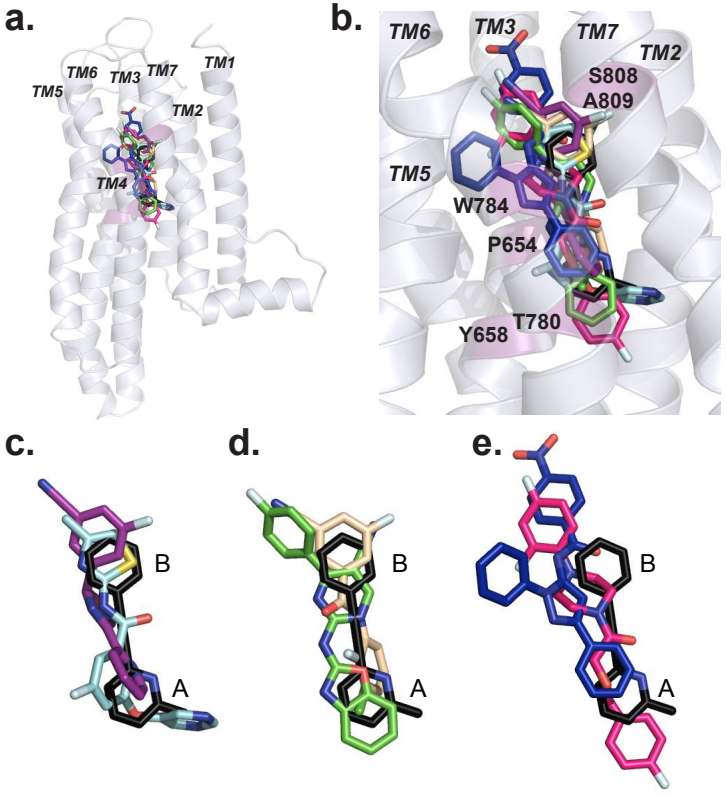

ACS Paragon Plus Environment

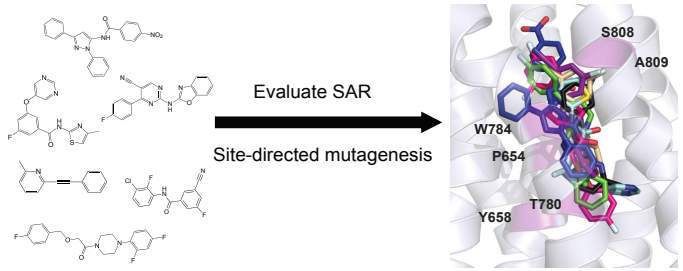

Title: Identification of specific ligand-receptor interactions that govern binding and cooperativity of diverse modulators to a common metabotropic glutamate receptor 5 allosteric site

Karen J. Gregory, Elizabeth D. Nguyen, Chrysa Malosh, Jeffrey L. Mendenhall, Jessica Z. Zic, Brittney S. Bates, Meredith J. Noetzel, Emma F. Squire, Eric M. Turner, Jerri M. Rook, Kyle A. Emmitte, Shaun R. Stauffer, Craig W. Lindsley, Jens Meiler and P. Jeffrey Conn.